Nuclear Materials and Energy 9 (2016) 571–575

Contents lists available at ScienceDirect

Nuclear Materials and Energy

journal homepage: www.elsevier.com/locate/nme

Atomistic simulations of deuterium irradiation on iron-based alloys in future fusion reactors

E. Safi[a,*], J. Polvi[a], A. Lasa[b], K. Nordlund[a]

[a] Association EURATOM-Tekes, University of Helsinki, PO Box 43, 00014 Helsinki, Finland
[b] Oak Ridge National Laboratory, Oak Ridge, TN 37831-6169, USA

ARTICLE INFO

Article history:
Received 13 November 2015
Revised 26 August 2016
Accepted 29 August 2016
Available online 14 October 2016

ABSTRACT

Iron-based alloys are now being considered as plasma-facing materials for the first wall of future fusion reactors. Therefore, the iron (Fe) and carbon (C) erosion will play a key role in predicting the life-time and viability of reactors with steel walls. In this work, the surface erosion and morphology changes due to deuterium (D) irradiation in pure Fe, Fe with 1% C impurity and the cementite, are studied using molecular dynamics (MD) simulations, varying surface temperature and impact energy. The sputtering yields for both Fe and C were found to increase with incoming energy. In iron carbide, C sputtering was preferential to Fe and the deuterium was mainly trapped as D_2 in bubbles, while mostly atomic D was present in Fe and Fe–1%C. The sputtering yields obtained from MD were compared to SDTrimSP yields. At lower impact energies, the sputtering mechanism was of both physical and chemical origin, while at higher energies (>100 eV) the physical sputtering dominated.

1. Introduction

One of the major challenges for future fusion reactors is the development of materials that will withstand the intense flow of a high energy plasma, due to non-perfect plasma confinement [1]. Various steels are being considered as plasma-facing materials (PFMs) for the main wall of DEMO, the main power-plant scale fusion reactor project [2]. The interest to this possibility was raised in particular by the recent realization that steels that have been made to have reduced activation by adding W, can have strongly reduced erosion due to preferential sputtering causing W enrichment at the surface [3]. However, for a steel to be viable as a PFM, certain qualities must be met, the most crucial issue is the lifetime of the steel, strongly affected by different erosion mechanisms. Since steels are alloys of iron (Fe) and carbon (C) (for instance, in the EUROFER steels planned to be used in DEMO, the carbon content is about 0.5 atomic % [4]), it is of vital importance to quantify the erosion of both elements when being exposed to hydrogen plasma, such as deuterium (D). Moreover, since steels in general have a complex microstructure and may contain, in addition to the basic iron phases, like austenite and ferrite, also carbide in layer and particles [5], it is also important to understand the sputtering of iron carbides.

Several experiments have been carried out to study sputtering of pure iron and that of steel containing some carbon over a wide range of irradiation energies [6,7]. However, little attention has been drawn to plasma-surface interactions (PSIs) of steel targets exposed to D plasma, and the preferential sputtering and depletion of C. In order to gain insight into the atomic processes and to make an assessment about the possible role of steel as PFM candidate, atomistic simulations are required.

In this work, we used molecular dynamics (MD) simulations to analyze the effect of D irradiation on ferrite, pure body-centered cubic (BCC) Fe, Fe with 1% C impurity (Fe–1%C) and the iron carbide (Fe_3C), under different irradiation energies and substrate temperatures. Since chemical effects during ion irradiations can be studied with MD, we compared our results to sputtering yields calculated with the dynamic binary collision approximation (BCA) code SDTrimSP [8]. Special attention was paid to sputtering behavior of C in Fe_3C.

2. Method

2.1. Molecular dynamics simulations

Molecular dynamics (MD) simulations is a computational method capable of describing bond formation and breaking when

* Corresponding author.
E-mail address: elnaz.safi@helsinki.fi (E. Safi).

http://dx.doi.org/10.1016/j.nme.2016.08.021

Table 1
Set-up characteristics of the molecular dynamics simulations, for pure iron (Fe), 1%-carbon (C) containing Fe and iron carbide (Fe_3C). The table specifies the number of atoms in the initial MD structure (N), the size of the initial structure, the surface temperature (T), the ion impact energy (E) and flux.

Structure	Fe	Fe–1%C	Fe_3C
N	3200	3232	2000
Size (nm)	$2.9 \times 2.9 \times 4.6$	$2.9 \times 2.9 \times 4.6$	$2.5 \times 3.8 \times 2.3$
T (K)	300, 400, 500, 600, 800	500	500
E (eV)	30, 40, 50, 70, 100, 200, 500	20, 40, 50, 70, 100, 150, 200	20, 40, 50, 70, 100, 150, 200
Flux (10^{28} m^{-2} s^{-1})	1.2	1.2	1.36

suitable reactive interatomic potentials are used. Consequently, it is an excellent tool for studying the erosion of chemically active structures. The code PARCAS [9] was used for MD simulations presented in this work. An analytical bond-order potential [10] was used to calculate interatomic forces in the binary Fe-D systems. To model the ternary Fe–C–D systems, the potential calculation was modified in such a way that C–C, C–D and D–D parameters are given by Brenner's second parametrization [11], while for bonds involving Fe atoms, the Fe–C potential [12] was used. Moreover, the formalism of Fe-C-D potential is based on formulation by Tersoff [13] and Brenner, and it has been shown to be suitable for describing both metallic and covalent bonds [14].

The MD simulations were carried out in two main steps: first the initial structure for pure Fe, Fe–1%C and Fe_3C was prepared, after which the cell was irradiated with 5000 cumulative D irradiations for pure (110) BCC Fe and Fe–1%C, and 3000 cumulative D irradiations for Fe_3C at normal incidence angle.

The initial simulation cells were created by relaxing the structures at the desired temperature, and opening a perfectly flat surface normal to the z-direction. In the Fe–1%C, the C atoms were inserted in randomly selected octahedral sites. After the relaxation, these surfaces were irradiated with cumulative D impacts varying the impact energy and substrate temperature. Each D impact simulation lasted for 7 ps.

Further details regarding to methodology, such as temperature and pressure control, use of electronic stopping and periodic boundary conditions can be found in Ref. [15]. The characteristics of each simulation cell and D ion parameters are listed in Table 1.

2.2. SDTrimSP

SDTrimSP is a BCA code suitable for simulation of atomic collisions in structure-less targets. In this work, SDTrimSP simulations were performed to provide comparison to the MD results. Fe_3C substrate was subjected to D ions with 50, 100, 150 and 200 eV energy. The fluence in all simulations was set to be 5×10^{16} m^{-2} .

It should be noted that in SDTrimSP no chemical effects are taken into account, therefore, the BCA approximation becomes unreliable at impact energies lower than 50 eV for heavy materials [16] like Fe and C. However, the code is reliable at high energies, and comparing the results with MD, where chemical effects have been taken into account, can provide important information about the underlying mechanisms.

3. Results and discussion

3.1. Pure Fe and Fe–1%C surfaces

Fig. 1 shows the total Fe sputtering yield as a function of surface temperature and D impact energy. Over all, the sputtering yield increases with the impact energy above 100 eV, the yields rapidly increase, as more kinetic energy is available for bond breaking. At impact energies above 200 eV, the yields begin to saturate.

The sputtering yields shown in Fig. 1 have no significant temperature (T) dependence within the range studied here. Therefore,

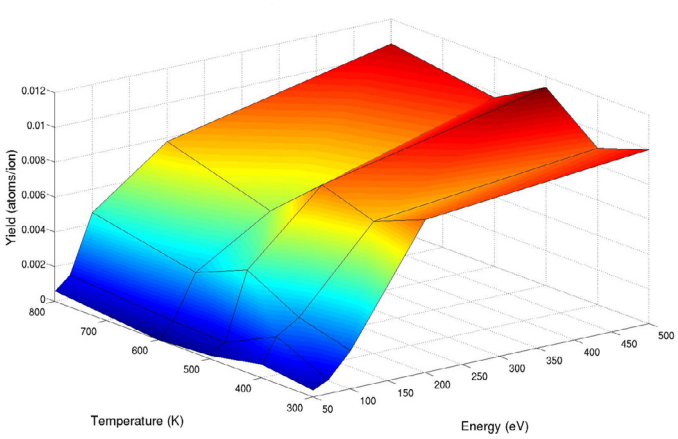

Fig. 1. Total Fe sputtering yield as a function of surface temperature and impact energy after 5000 cumulative D impacts for pure Fe.

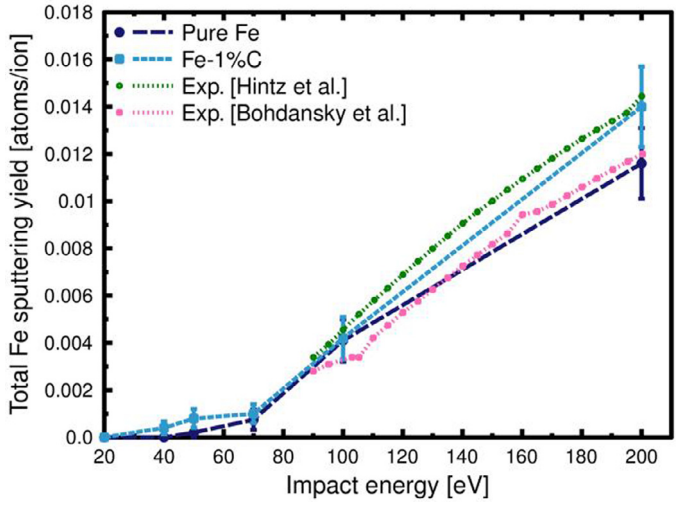

Fig. 2. A comparison of Fe sputtering yields in pure Fe and Fe–1%C between MD simulations and experimental data at different impact energies. In the simulations, the temperature was set to 500 K.

and due to limitations in available computational resources, the rest of simulations were carried out at T = 500 K, with varying D impact energy. Fe molecular sputtering was found to be negligible in these simulations.

In Fig. 2, Fe sputtering yields for pure Fe, and for Fe–1%C are compared to the experimental outcome by Hintz et al. [7] and by Bohdansky et al. [6], for D impact energies between 90 and 200 eV The results show excellent agreement between simulations and experiments.

Fig. 3 shows the fraction of D atoms not implanted in the pure Fe, and the Fe–1%C, simulations cells. Those atoms were either reflected from the surface or released as molecules. The figure shows

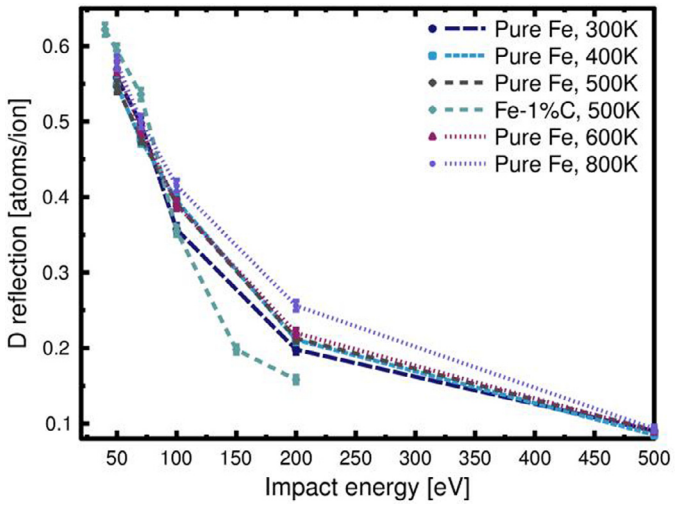

Fig. 3. D reflection on pure Fe at different temperatures and Fe–1%C as a function of energy, obtained after 5000 cumulative D impacts.

that the fraction of reflected atoms decreases as the impact energy increases. For D impact energies higher that 100 eV, a significant fraction of the bombarded D went through the simulation cell. In general, D atoms were mostly either retained in the bulk or reflected as single D atoms. Release of molecular D was found to be minor. Moreover, in the Fe–1%C simulation cell, C impurities were found to trap more D, which resulted in slightly lower D reflection than in the pure Fe simulation at 500 K. The effect of surface temperature for D implantation in pure Fe was found to be negligible. It might be worth further study to look more deeply into sputtering with 200–500 eV energy range as well as repeat the simulations with other temperatures for Fe–1%C.

3.2. Iron carbide, Fe_3C

As shown in Fig. 4, Fe_3C lattice loses its crystallinity in the D rich areas, and the fraction of amorphous volume increases with increasing D fluence. The observation of amorphization is well in line with previous MD simulations of continuous irradiation of cementite with Fe recoils [17]. Further, the erosion is not homogeneous, leading to surface roughening.

At impact energies higher than 70 eV, D was implanted deeper into the substrate, forming bubbles of D_2 molecules. For even higher energies, we anticipate to see the same effect that was observed in tungsten carbide [18], where with increasing D fluence, the D_2 accumulation would result in a blistering-like effect; the top layer would fly off due to the high gas pressure. It should be noted that the higher C content facilitates the formation of D_2 molecules in the system.

At higher impact energies, incoming D ions kicked C atoms from their lattice sites to the surface, while next D ions transferred their kinetic energy to these surface atoms, causing sputtering.

In general, D atoms did not bond to C atoms, and only small number of hydrocarbons were observed in our simulations.

Fig. 5 illustrates the fraction of D atoms reflected from the surface of Fe_3C, as a function of impact energy. The fraction of reflected atoms decreases as the impact energy increases, and the trend is very similar to cases of pure Fe and Fe–1%C shown in Fig. 3. At $E = 20$ eV, over 90% of D ions were backscattered from the surface.

Fig. 6 illustrates total Fe and C sputtering yields for Fe_3C by MD and SDTrimSP. In general, sputtering yields for both atom types increased with incoming ion energy. For energies lower than 100 eV, C sputtering was higher in MD than in SDTrimSP, and for higher ion energies MD and SDTrimSP match within the margin of error. Since SDTrimSP simulates only physical sputtering, these results suggest that both chemical and physical sputtering are present for ion energies below 100 eV, and that for higher energies, sputtering was mostly of physical origin, rather than swift chemical sputtering (SCS) [19].

Table 2
The number of each sputtered species after 3000 cumulative D impacts on Fe_3C at different energies.

Energy(eV)	N sputtered species
20	1 CD
40	16 C, 3 CD, 1 FeC, 2 Fe, 1 FeD, 1 FeD_2, 1 FeD_3
50	28 C, 1 CD, 6 Fe
70	28 C, 1 CD, 1 FeC, 1 Fe_2C, 1 FeC_2, 4 Fe, 2 FeD
100	37 C, 7 Fe, 2 FeD
150	36 C, 1 C2, 1 FeC_2, 20 Fe, 3 FeD, 1 FeD_2
200	41 C, 3 CD, 1 CD_3, 1 C_2D_2, 1 CFe, 44 Fe, 1FeD

In MD, the C sputtering yields are larger than Fe sputtering yields due to preferential C sputtering from carbide surfaces, specially in the 40–150 eV range. The SDTrimSP results give somewhat higher Fe sputtering yields than MD, indicating that the surface binding energies are not quite suitable for cementite.

The sputtered atoms and molecules from our Fe_3C simulations are shown in Table 2. The sputtered C atoms were mainly in atomic form for ion energies higher than 40 eV, and, similarly, Fe sputtered mostly in atomic form for ion energies 50 eV and above. On the whole, the number of sputtered molecules was 10–20% of the total number of sputtered species for ion energies above 40 eV, few hydrocarbons were sputtered (Table 2). The presence of acetylene molecules within the sputtered species gives us confidence that the potential used here offers a reasonable description of the C-D chemistry.

The number of Fe atoms in the MD simulation samples as a function of the number of cumulative impacts are given in Fig. 7(a) at different impact energies. Fe is eroded linearly with the number of impacts and the slope is constant over the whole irradiation range. Fig. 7(b) shows the number of C atoms in the sample, indicating that C erosion slows down after 1500 bombardments, with the exception of 200 eV ion energy case, which remains mostly linear. This change is due to the surface layers of the simulation cells having become depleted of C due to preferential sputtering.

4. Conclusion

Using MD simulations, we studied the effect of D irradiation on iron-based alloys, varying the substrate temperature (300–800 K) and impact energy (20–500 K). We found that while Fe sputtering yield had a positive correlation with impact energy, the effect on substrate temperature, for the surface studied here was negligible.

In Fe_3C, due to preferential sputtering of C during the bombardment, the surface was enriched with Fe. Analyzing the sputtering mechanism of Fe and C showed that it is dominantly of physical origin at impact energies higher than 100 eV With impact energies up to 100 eV, C sputtering dominated over Fe sputtering. Increasing the impact energy from 100 eV brought the sputtering yields from C and Fe closer, and with 200 eV the yields were equal within the margin of error.

We found that the number of implanted D ions vs. the number of reflected D ions varied greatly with the impact energy, and that the trapped D in iron-based carbon-containing alloys forms D_2 molecules. Furthermore, the initial lattice structure was observed to become completely amorphised at the D implantation zone.

In general, our results show that if steels are used as a plasma-facing material, the presence of C in them will lead to chemical sputtering of carbon-containing molecules. Carbon transport

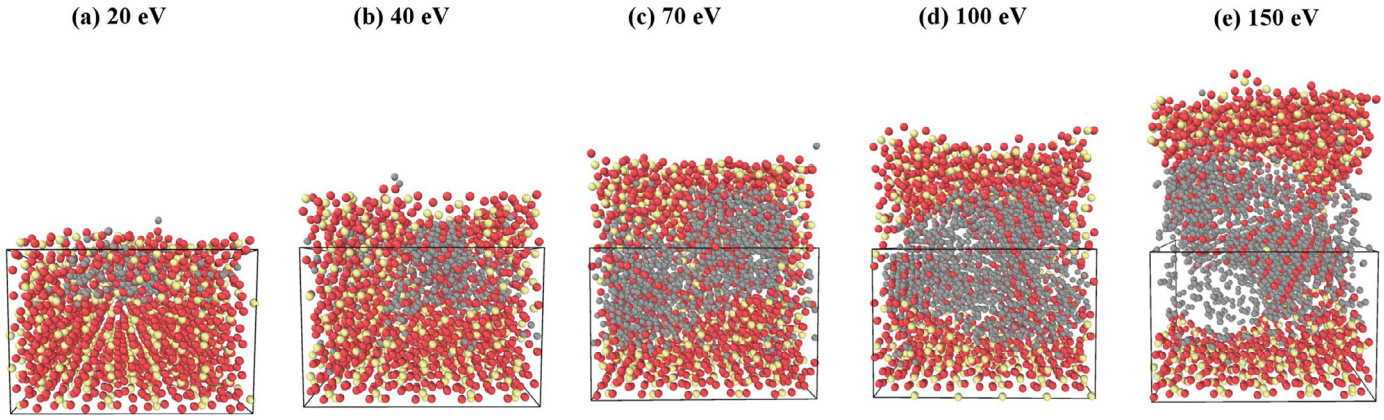

Fig. 4. Structure of Fe_3C after 3000 D impacts with different energies, for a substrate temperature of 500 K. Red, yellow and gray spheres represent Fe, C and D atoms, respectively. (For interpretation of the references to color in this figure legend, the reader is referred to the web version of this article.)

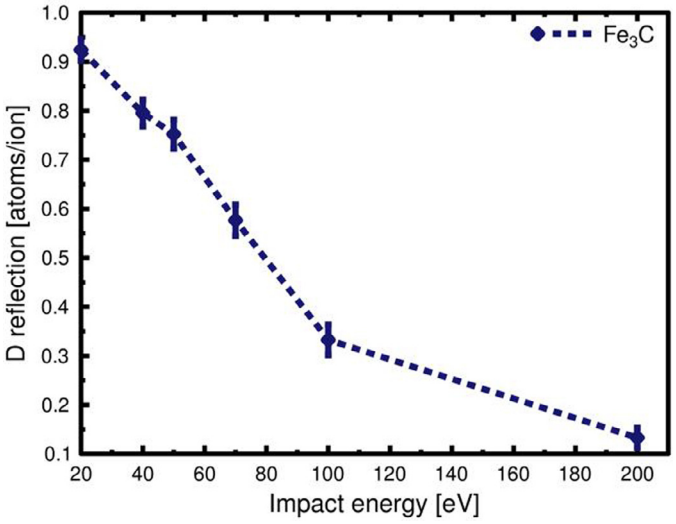

Fig. 5. D reflection from Fe_3C as a function of energy at T = 500 K, obtained after 3000 cumulative D impacts.

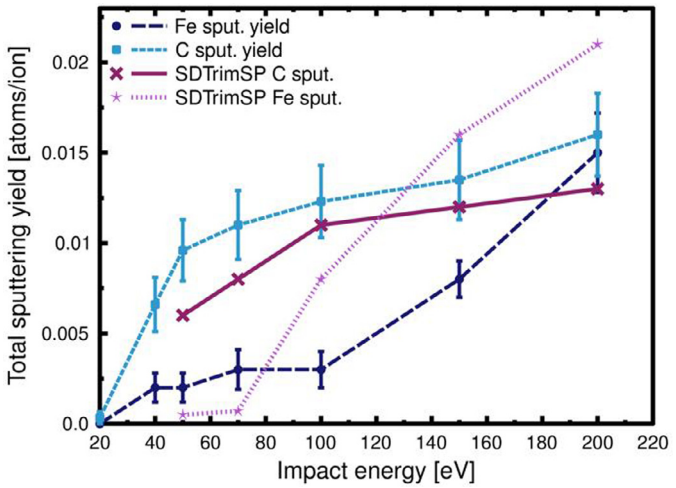

Fig. 6. Total Fe and C sputtering yield as a function of impact energy of Fe_3C erosion by 3000 cumulative and 100,000 non cumulative D irradiations for MD and SDTrimSP simulations, respectively.

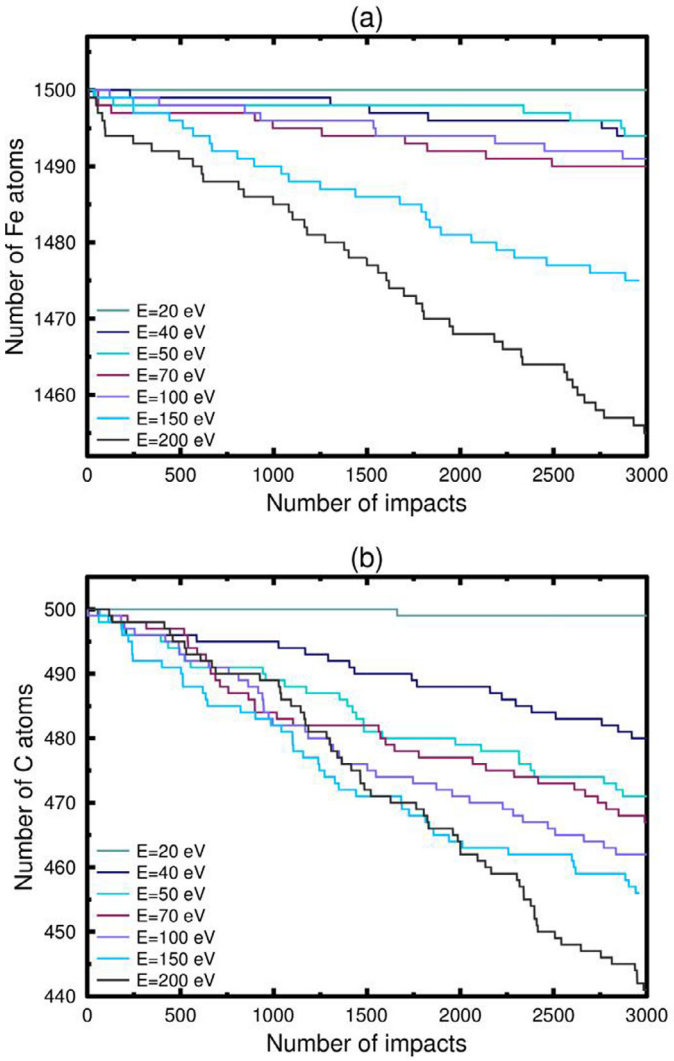

Fig. 7. Number of Fe (a) and C atoms (b) in the Fe_3C cell as a function of number of impacts at different impact energies for 3000 cumulative D irradiations.

and inventory calculations will be required to assess whether this will during prolonged operation lead to redeposition of significant amounts of carbon, and specifically carbon-bound tritium, elsewhere in the reactor.

Acknowledgments

This work has been carried out within the framework of the EUROfusion consortium and has received funding from the Euratom research and training program 2014–2018 under grant agreement No. 633053. The views and opinions expressed herein do not necessarily reflect those of the European commission. Grants for computer time from CSC, the IT center science in Espoo, Finland, are gratefully acknowledged.

References

[1] R.K. Janev, Atomic and Molecular Processes in Fusion Edge Plasmas, 1995, pp. 1–13.
[2] D. Stork, et. al., Developing structural, high-heat flux and plasma facing materials for a near-term DEMO fusion power plant: the EU assessment, 2014. http://www.ccfe.ac.uk/assets/Documents/CCFE-PR(14)08.pdf
[3] J. Roth, K. Sugiyama, V. Alimov, T. Hoeschen, M. Baldwin, R. Doerner, J. Nucl. Mater. 454 (2014) 1–6.
[4] C.A. Williams, E.A. Marquis, A. Cerezo, G.D. Smith, J. Nucl. Mater. 400 (2010) 37–45.
[5] W.D. Callister Jr., Materials Science and Engineering, An Introduction, Wiley, 1993.
[6] J. Bohdansky, H.L. Bay, J. Roth, J. Appl. Phys. 51 (1980) 2861.
[7] R. Behrisch, J. Roth, J. Bohdansky, A.P. Martinelli, B. Schweer, D. Rusbüldt, E. Hintz, J. Nucl. Mater. 93-94 (1980) 645–655.
[8] W. Eckstein, R. Dohmen, A. Mutzke, R. Schneider, SDTrimSP: A Monte-Carlo Code for Calculating Collision Phenomena in Randomized Targets, 2007 IPP Reports 12/3.
[9] K. Nordlund, 2006, PARCAS computer code.
[10] P. Kuopanportti, E. Hayward, C. Fu, A. Kuronen, K. Nordlund, Comput. Mater. Sci. 111 (2016) 525–531.
[11] D.W. Brenner, Phys. Rev. B 42 (1990) 9458.
[12] K.O.E. Henriksson, C. Björkas, K. Nordlund, J. Phys. Condens. Matt. 25 (2013) 445401.
[13] J. Tersoff, Phys. Rev. B 37 (1988) 6991.
[14] K. Albe, K. Nordlund, R.S. Averback, Phys. Rev. B 65 (2002) 195124.
[15] K. Vörtler, K. Nordlund, J. Phys. Chem. C 114 (2010) 5382–5390.
[16] G. Hobler, G. Betz, On the useful range of application of molecular dynamics simulations in the recoil interaction approximation, Nucl. Instr. Methods B 180 (2001) 203–208.
[17] K.O.E. Henriksson, K. Nordlund, Nucl. Instr. Meth. Phys. Res. B 338 (2014) 119.
[18] K. Vörtler, C. Björkas, K. Nordlund, J. Phys. 23 (8) (2010) 085002.
[19] C. Björkas, K. Vörtler, K. Nordlund, D. Nishijima, R. Doerner, New J. Phys. 11 (2009) 123017.